

Reinforcement Learning with Foundation Priors: Let the Embodied Agent Efficiently Learn on Its Own

Weirui Ye¹²³ Yunsheng Zhang²³ Haoyang Weng¹ Xianfan Gu² Shengjie Wang¹²³
Tong Zhang¹²³ Mengchen Wang¹ Pieter Abbeel⁴ Yang Gao^{123 *}

¹Tsinghua University, ²Shanghai Qi Zhi Institute
³Shanghai Artificial Intelligence Laboratory, ⁴UC Berkeley

Abstract: Reinforcement learning (RL) is a promising approach for solving robotic manipulation tasks. However, it is challenging to apply the RL algorithms directly in the real world. For one thing, RL is data-intensive and typically requires millions of interactions with environments, which are impractical in real scenarios. For another, it is necessary to make heavy engineering efforts to design reward functions manually. To address these issues, we leverage foundation models in this paper. We propose Reinforcement Learning with Foundation Priors (RLFP) to utilize guidance and feedback from policy, value, and success-reward foundation models. Within this framework, we introduce the Foundation-guided Actor-Critic (FAC) algorithm, which enables embodied agents to explore more efficiently with automatic reward functions. The benefits of our framework are threefold: (1) *sample efficient*; (2) *minimal and effective reward engineering*; (3) *agnostic to foundation model forms and robust to noisy priors*. Our method achieves remarkable performances in various manipulation tasks on both real robots and in simulation. Across 5 dexterous tasks with real robots, FAC achieves an average success rate of 86% after one hour of real-time learning. Across 8 tasks in the simulated Meta-world, FAC achieves 100% success rates in 7/8 tasks under less than 100k frames (about 1-hour training), outperforming baseline methods with manual-designed rewards in 1M frames. We believe the RLFP framework can enable future robots to explore and learn autonomously in the physical world for more tasks.

Keywords: Reinforcement Learning, Foundation Models, Robotics

1 Introduction

Reinforcement Learning (RL) has achieved remarkable success in various domains, including video games [1, 2, 3], simulated robotics [4], demonstrating significant potential in solving decision-making tasks. Researchers have been increasingly applying RL algorithms to embodied agents for decades, such as real robots [5, 6, 7, 8, 9]. However, current RL algorithms encounter two primary challenges: sample efficiency and heavy reward engineering, which hinder deployment in the real world. For example, researchers [1, 10] require millions of data to master Go and Atari games, and current methods require millions of frames to solve simulated robotics tasks [11, 12, 13]. Such amounts of data are unaffordable in real. The success of current RL methods depends on manually designed rewards, which is overly burdensome. Therefore, it is essential to address these two issues.

Humans are capable of acquiring skills through minimal interactions with the environment by leveraging the innate abilities and abundant commonsense accumulated in daily life. They will start from some reasonable behaviors with fewer aimless explorations, make adjustments as well as corrections, and reinforce successful behaviors. We take the baby pressing bottom as an example, which is commonly used in psychology [14, 15], to illustrate this learning paradigm. As shown in Fig. 1, a baby named Alice is presented with a novel toy box with a button. The baby observes an adult

*Corresponding author. Emails: ywr20@mails.tsinghua.edu.cn; gaoyangjiis@tsinghua.edu.cn.

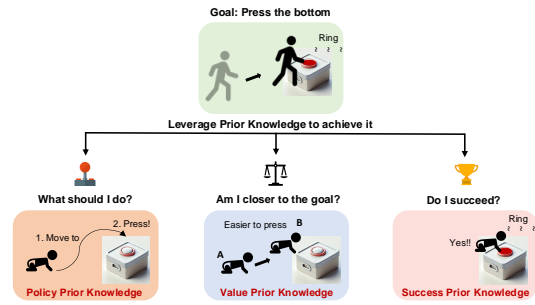


Figure 1: An example of how human solves tasks under the policy, value, and success-reward prior knowledge. The proposed **Reinforcement Learning from Foundation Priors** framework utilizes the corresponding foundation models to acquire prior knowledge.

pressing the button, causing the toy box to light up and make a sound. Alice knows the rough behavior to accomplish the task, e.g., pressing the button to activate the toy. And she realizes that she can make it easier by positioning the hand closer to the button. Once she sees the toy box light up and hears the sound, she will reinforce the successful trial and repeat it in future trials.

Inspired by such a learning paradigm, we explore the use of various foundation models to provide learning signals and enhance learning efficiency. Then two fundamental challenges arise: (1) what is the concrete form to present prior knowledge for RL; (2) how to leverage the corresponding prior knowledge effectively for downstream tasks. Based on how humans complete the new task shown in Fig. 1, there are three kinds of prior knowledge that answer the questions: what should I do now? am I closer to the goal? did I succeed? Notably, these prior knowledge can be aligned with the core concepts well in the Markov Decision Process (MDP), which corresponds to the policy function, the value function, and the success-reward function. Fortunately, the great success of the foundation models in natural language processing [16, 17, 18, 19] and computer vision [20, 21, 22, 23] makes it possible to acquire considerable and informative prior knowledge for embodied agents.

Consequently, for systematically utilizing the abundant prior knowledge to facilitate the embodied agent efficiently learning on its own, we introduce the Reinforcement Learning from Foundation Priors (RLFP) to leverage policy, value, and success-reward prior knowledge. In this framework, the learning signals of RL are derived from corresponding foundation models. The policy prior gives a warm start behavior of the agent; the value prior informs to reach better states, and the success-reward prior gives the final success feedback.

To verify the efficacy of RLFP, we instantiate an actor-critic algorithm, named Foundation-guided Actor-Critic (FAC), inspired by some works about building foundation policy or value models [24, 25, 26]. We conduct experiments on real robots and in simulation. We make extensive ablations in simulation towards each component in our framework and different qualities of the foundation models. RLFP demonstrates three key benefits: (1) Sample efficient learning. Across the 5 dexterous tasks in real robots, FAC can achieve 86% success rates on average after 1 hour of learning in real. Across the 8 tasks in the simulated Meta-world, FAC can achieve 100% success rates in 7/8 tasks under less than 100k frames (about 1 hour of training). This performance surpasses baseline methods that rely on manually designed rewards over 1M frames. (2) Minimal and effective reward engineering. The reward function is derived from the value and success-reward prior knowledge, eliminating the need for human-specified dense rewards or teleoperated demonstrations. (3) Agnostic to prior foundation model forms and robust against noisy priors. Our framework can leverage various foundation models. Notably, to ensure high efficiency and performance, we utilize several well-trained foundation models or fine-tuning foundation models. Moreover, FAC demonstrates resilience even under heavy noise or quantization errors in simulations. The contributions are:

- We propose the Reinforcement Learning with Foundation Priors (RLFP) framework. It systematically introduces three priors that are essential to embodied agents, and suggests how to leverage the existing foundation models as the priors.
- We propose the Foundation-guided Actor-Critic (FAC), an RL algorithm under the RLFP framework that utilizes the policy, value, and success-reward prior knowledge.
- Empirical results demonstrate the remarkable performances of FAC. The ablations underscore the importance of each priors and validate the robustness against prior qualities.

2 Related Work

Foundation Models for Policy Learning. The ability to leverage generalized knowledge from large and varied datasets has been proved in the fields of CV and NLP. In embodied AI, researchers attempt to learn universal policies based on large language models (LLMs) or vision-language models (VLMs). Some researchers train large transformers by tokenizing inputs and inferring actions by imitation learning [27, 28, 29, 30], offline Reinforcement Learning [31], or fine-tuning the pre-trained VLMs [8] for downstream tasks. Some researchers utilize the LLMs or VLMs as reasoning tools and do low-level control based on language descriptions [32, 33, 34, 35, 36, 37, 38, 39]. The above works utilize human teleoperation to collect data for policy learning. However, it is hard to scale up human teleoperation to collect large-scale data. Some works generate code policies based on LLMs or VLMs [40, 41], while UniPi [25] predicts future videos from diffusion models [42] and generates actions via an inverse dynamics model. However, they are of poor robustness empirically because of a lack of interactions with the environments by generated codes or videos.

Foundation Models for Representation Learning. Apart from learning policies directly from the foundation models, some researchers attempt to extract universal representations for downstream tasks. Some works focus on pre-trained visual representations that initialize the perception encoder or extract latent states of image inputs [43, 44, 45, 46]. Some researchers incorporate the pre-trained LLMs or VLMs for linguistic instruction encoding [47, 48, 49]. Some have investigated how to apply the LLMs or VLMs for universal reward or value representation in RL. [50, 51, 52] build language-conditioned reward foundation models to generate task reward signals, and [24] is the first to train a universal goal-conditioned value function on large-scale unlabeled videos. Some works acquire value and success signals through human demonstrations [53, 54]. More researchers attempt to generate rewards under the value difference to avoid the design of reward functions [55, 8]. However, this learning paradigm presents certain limitations. Firstly, it lacks policy-side guidance, resulting in inefficient agent exploration. Secondly, the inferred values/rewards are continuous scalars with relatively high error and variance from the neural networks, leading to instability and difficulty in optimization. In contrast, our proposed framework leverages policy, value, and success-reward prior knowledge, which covers the abundant commonsense of solving decision-making tasks. In this way, our method is orthogonal to the current data-efficient RL algorithms [56, 11, 2, 57, 58, 59].

3 Method

This paper focuses on facilitating embodied agents to efficiently learn various tasks on their own. In Sec. 3.1, we introduce the definition and formulation of the proposed framework Reinforcement Learning with Foundation Priors (**RLFP**). Subsequently, in Sec. 3.2, we instantiate the Foundation-guided Actor-Critic (**FAC**) algorithm based on the proposed framework. Finally, we introduce how to acquire the corresponding foundation models in FAC in Sec. 3.3.

3.1 Reinforcement Learning with Foundation Priors

We model the tasks for embodied agents as the Goal-Conditioned Markov Decision Processes (GCMDP) \mathcal{G} : $\mathcal{G} = (\mathcal{S}, \mathcal{A}, \mathcal{P}, \mathcal{R}, \mathcal{T}, \gamma)$. $\mathcal{S} \in \mathbb{R}^m$ denotes the state. \mathcal{A} is the action space, which is the continuous delta movement of the end effector in this work. \mathcal{P} is the transition probability function. \mathcal{T} is the task identifier. \mathcal{R} denotes the rewards. γ is the discounting factor, which is equal to 0.99 in the paper. To solve the MDP, vanilla RL requires heavily reward engineering for different tasks and performs poorly under limited interactions with the environment. To enable the agent to learn efficiently and automatically, we propose the Reinforcement Learning from Foundation Priors (**RLFP**) framework by leveraging the policy, value, and success-reward priors.

Here we demonstrate how we formulate the corresponding priors in RLFP. Back to the case of Alice in Fig. 1, the commonsense of rough behavior can be formulated as a goal-conditioned policy function, $M_\pi(s, \mathcal{T}) : \mathcal{S} \times \mathcal{T} \rightarrow \mathcal{A}$. The prior knowledge that the state closer to the button is closer to success can be formulated as a goal-conditioned value function $M_V(s, \mathcal{T}) : \mathcal{S} \times \mathcal{T} \rightarrow \mathbb{R}^1$.

The ability to recognize the success state can be formulated as the 0-1 success-reward function $M_{\mathcal{R}}(s, \mathcal{T}) : \mathcal{S} \times \mathcal{T} \rightarrow \{0, 1\}$, which equals 1 only if the task succeeds. Notably, we assume the success-reward prior is relatively precise and sound, given the simplicity of binary classification in determining success. The value and policy prior knowledge can be much noisier. Conveniently, the RLFP framework is to solve an expansion of \mathcal{G} , termed $\mathcal{G}' = (\mathcal{G}, \mathcal{M})$, where \mathcal{M} is the foundation model set that represents various foundation prior knowledge. Here, $M_{\pi}, M_V, M_{\mathcal{R}} \in \mathcal{M}$.

Compared to vanilla RL, all the signals for the RLFP should come from the foundation models. The vanilla RL relies on uninformative trial and error explorations as well as carefully and manually designed reward functions to learn the desired behaviors. It is not only of poor sample efficiency but also requires lots of human reward engineering. Instead, in RLFP, the prior knowledge from the foundation model set \mathcal{M} can provide guidance or feedback in the aspects of policy, value, and success-reward, which enables automatic and more effective task resolution.

3.2 Foundation-guided Actor-Critic

Under the proposed RLFP framework, we instantiate an actor-critic algorithm named Foundation-guided Actor-Critic (FAC), demonstrating how to inject the three priors into RL algorithms.

Guided by Success-reward Signals. Generally, we consider the given task as MDP \mathcal{G}_1 with 0-1 success-rewards, where $\mathcal{R}_{\mathcal{G}_1} = M_{\mathcal{R}}(s, \mathcal{T}) \in \{0, 1\}$. Moreover, following the conception that human can learn from their successful trials, we propose to build a success buffer to store the previous “successful” trajectories discriminated by $M_{\mathcal{R}}$ during exploration. Each time the actor π_{ϕ} is updated through the policy gradient, it will also imitate a batch of sample data from the success buffer $\mathcal{D}_{\text{succ}}$ (if there exists data). The objective is $\mathcal{L}_{\text{succ}}(\phi) = \mathbf{KL}(\pi_{\phi}(s_t), \mathcal{N}(a_t, \hat{\sigma}^2))$, $s_t, a_t \sim \mathcal{D}_{\text{succ}}$, where $\hat{\sigma}$ is the standard deviation hyper-parameter. It allows agents to reinforce the successful trajectories. Moreover, we utilize the policy and value prior knowledge to solve the task more efficiently.

Guided by Policy Regularization. To encourage the embodiment to explore the environments with the guidance of policy prior knowledge, we regularize the actor π_{ϕ} by the policy prior from $M_{\pi}(s, \mathcal{T})$ during training. Without loss of generality, we assume that the policy foundation prior follows Gaussian distributions. Thus, the regularization term is $\mathcal{L}_{\text{reg}}(\phi) = \mathbf{KL}(\pi_{\phi}, \mathcal{N}(M_{\pi}(s_t, \mathcal{T}), \hat{\sigma}^2))$. Such regularization is simple to implement but effective, which is widely used in other algorithms [60, 61]. The bias caused by the policy prior can be bounded theoretically in Theorem 2.

Guided by Reward-shaping from Value Prior. The noisy foundation policy prior might mislead agents to undesired states. We propose to guide the policy by the value model M_V to avoid unnecessary exploration of unpromising states. A natural approach is initializing with $M_V(s, \mathcal{T})$ and fine-tuning the value functions. However, we empirically find that it performs poorly due to catastrophic forgetting issues. To better employ the value prior, we propose to utilize the **reward-shaping** technique [62]. We introduce the potential-based shaping function $F(s, s', \mathcal{T}) = \gamma M_V(s', \mathcal{T}) - M_V(s, \mathcal{T})$, where γ is the discounting factor. Intuitively, since M_V roughly estimates the state values, F can measure the increase of value towards reaching the next state s' from the current state s . The shaping reward will be positive if s' is better than s . Meanwhile, it shares the same optimal solution as the vanilla 0-1 success-reward MDP \mathcal{G}_1 , under the potential-based shaping function F . The optimality proof and more details about reward shaping are attached in App. A.1.

Foundation-guided Actor-Critic. In summary, we propose to deal with a new MDP \mathcal{G}_2 , where $\mathcal{R}_{\mathcal{G}_2} = \lambda M_{\mathcal{R}} + F$, $\lambda > 0$. Here, the λ emphasizes the success feedback, which equals 100 in this

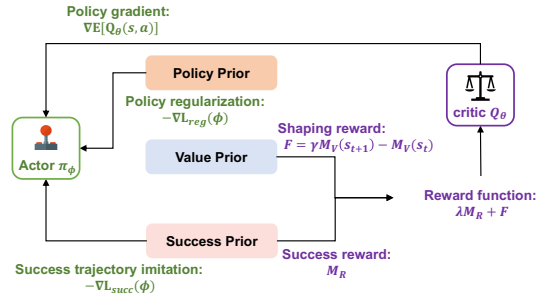


Figure 2: **The overview of Foundation-guided Actor-Critic.** In FAC, reward signals come from foundation success rewards and foundation value shaping. In addition to policy gradient signals, the actor is learned by the prior policy regularization and the success trajectory imitation.

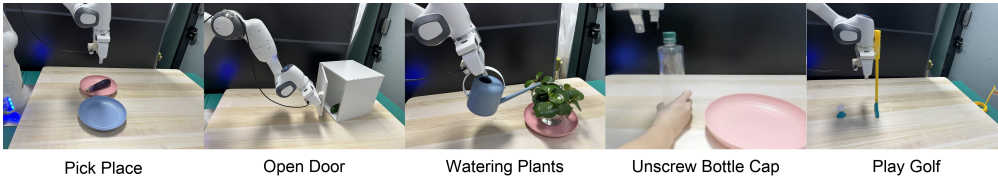


Figure 3: Five tasks on real robots, demonstrating the efficiency and accuracy of FAC in real.

work. We train the agent based on DrQ-v2 [11], a variant of Actor-Critic algorithms. We name the proposed RLFP method as Foundation-guided Actor-Critic (**FAC**), shown in Fig. 2. FAC learns from foundation policy guidance and the automatic reward function. Thus, the embodied agent can efficiently learn on its own based on the abundant prior knowledge. The objectives of FAC are listed in Eq. (1), where α, β as the tradeoffs are both set to 1, y is the n -step TD target value, and $Q_{\hat{\theta}}$ is the target network. We employ clipped double Q-learning [63] to reduce the overestimation.

$$\begin{aligned} \mathcal{L}_{\text{actor}}(\phi) &= -\mathbb{E}_{s_t \sim \mathcal{D}} \left[\min_{k=1,2} Q_{\theta_k}(s_t, a_t) \right] + \alpha \mathcal{L}_{\text{succ}} + \beta \mathcal{L}_{\text{reg}}; a_t \sim \pi_{\phi}(s_t) \\ \mathcal{L}_{\text{critic}}(\theta) &= \mathbb{E}_{s_t \sim \mathcal{D}} \left[(Q_{\theta_k}(s_t, a_t) - y)^2 \right]; y = \sum_{i=0}^{n-1} \gamma^i r_{t+i} + \gamma^n \min_{k=1,2} Q_{\hat{\theta}_k}(s_{t+n}, a_{t+n}) \end{aligned} \quad (1)$$

3.3 Acquiring Foundation Prior in FAC.

We aim to study how to leverage Foundation Priors in RL, so building large-scale foundation models is out of our paper’s scope. However, we think it is an exciting future research direction. To achieve remarkable performance, we suggest well-trained or pre-trained foundation models. Here, we utilize several existing works as proxy foundation models. We choose the GPT-4V as the success-reward foundation model $M_{\mathcal{R}}$ for the real tasks. Due to the poor performance of GPT-4V in sim, we use the ground-truth 0-1 success reward in sim and distill a noisy success reward function for ablations. We utilize the VIP model [24] as the value foundation model $M_{\mathcal{V}}$, which takes in the current image observation and goal image observation to predict the value. We build the prior policy M_{π} by code generation [40, 41] or under video diffusion models [25]. We will introduce the details of each in the next section, and more details are in App. A.3.1 and App. A.3.2.

4 Experiments

In this section, we present detailed evaluations of the Foundation-guided Actor-Critic (FAC) on robotics manipulation tasks, encompassing both real-world and simulated environments. Additionally, we explore the impact of foundation prior knowledge through ablations in simulation, specifically focusing on sample efficiency and robustness. Our experiments are designed to address the following questions: **(a)** How sample efficient is the FAC algorithm, in Sec. 4.1 and Sec. 4.2; **(b)** What is the individual significance of the three foundation priors, in Sec. 4.3; **(c)** How does the quality of the foundation model influence the performance of FAC, in Section 4.3. More Ablations are included in App. A.5, and the running time analysis of foundation priors is in App. A.4. Demo real-world videos and generated videos from the diffusion model are attached in the supplementary.

4.1 Manipulation tasks on Real Robots

Experimental Setup. We established a real-world tabletop environment using a Franka Emika Panda robot, which is equipped with a 7-degree-of-freedom (DoF) arm and a 1-DoF parallel jaw gripper. Observations are obtained from RGB images captured by both a fixed external camera and a wrist-mounted camera on the robot. We design five dexterous manipulation tasks to evaluate the performance of FAC, as illustrated in Fig. 3. The agent undergoes an hour of learning with the environments for these tasks, except for the "Pick Place" task, which involves a training period of 30 minutes. The numbers of collected real-world trajectories of the tasks Pick Place, Open Door, Watering Plants, Unscrew Bottle Cap, and Play Golf are 40, 75, 60, 50, and 115 respectively. These tasks are designed to exhibit the necessity for leveraging prior knowledge to accurately manipulate the objects, which can be hard for vanilla RL. For each task, the starting position of the Franka Arm remains fixed, while the positions of objects vary within a predefined range across different trajectories. And we evaluate them across 10 distinct trajectories under small variations in the environment. Further training details are provided in App. A.2.

Table 1: **Quantitative Results of FAC during One-Hour Learning on the Franka Arm.** The reported results are based on 10 evaluation trials. FAC achieves 86% success rate on average after one hour of training. This performance notably surpasses the code policy prior, underscoring its efficiency.

Task (Succ.)	Pick Place	Open Door	Watering.	Unscrew.	Play Golfs	Avg.
Vanilla RL	0.00	0.00	0.00	0.00	0.00	0.0
Code Policy	0.30	0.10	0.30	0.20	0.20	0.22
FAC	1.00	0.90	0.80	0.90	0.70	0.86

Acquiring Foundation Prior. (1) Prior success-reward. We employ GPT-4V to automatically determine the success-reward. For efficiency, each task maintains a consistent episodic length, with only the final observation being evaluated for success determination. To assess the accuracy of GPT-4V, we sampled 20 trajectories for each task. Remarkably, the results demonstrate GPT-4V’s robustness in correctly identifying success states, with no recorded false negatives or false positives. The exception is the Watering Plants task, where the false-positive rate was 25%. This is attributed to the task’s specific requirement: successful watering occurs only when the spout orients towards the plants horizontally, which is more challenging. Overall, GPT-4V can serve as an effective proxy model for acquiring success-reward prior knowledge. (2) Prior policy. We explore GPT-4V to make code generations for the initial state. Following previous works [40, 41, 34], we provide some primitive low-level skills, such as move_to, grasp, release, rotate_anticlockwise, etc, including the usage and the parameters of the functions. It is an executable code that takes as input the current robot state and outputs an action based on the configuration and the current state. The code policy can output a prior action based on the robot’s state. Therefore, we can take the KL loss between the policy and prior policy actions on non-initial states (3) Prior value. We load the VIP [24] model, which is a universal value model trained on some internet-scale datasets. We input the goal observation and the current observation to infer the value of the state. Demonstrations of the prompts, the generated policy, and the setting details of each prior are available in App. A.3.1.

Efficient and Safe Exploration on Real Robots. To achieve higher sample efficiency on real robots, we choose high update-to-data (UTD) ratios with layer normalization in all MLP layers [64]. To achieve safer exploration, we introduce two key modifications. Firstly, we warm up the learning by taking the prior action to gather the first 10 trajectories. Secondly, under the guidance of critics, we selectively choose the superior action $a^* = a_i$ from either the actor π_ϕ or the policy prior M_π , where $i = \arg \max_{i \in \{1, 2\}} [\min_k Q_{\theta_k}(s, a_i)]$, $a_1 \sim \pi_\phi$, $a_2 \sim M_\pi$. As training progresses, the agent increasingly opts for the actor’s actions over the prior, shown in Fig. 4. For the actor, we maintain a constant standard deviation of 0.1.

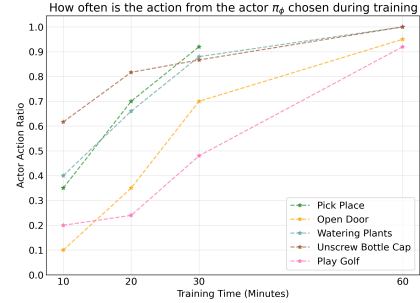


Figure 4: During training, the agent progressively favors actions from the actor, reducing reliance on the prior policy.

Baselines and Performance Analysis in Real.

On real robots, we compare our method to the following baselines: (1) Vanilla RL, utilizing DrQ-v2 [11] with manually designed rewards; (2) Policy Prior, which executes the code policy generated from GPT-4V. The results are in Tab. 1. We find that learning from scratch under the vanilla RL fails in all tasks in one hour of training, because it experiences large amounts of aimless exploration. The code policy prior can achieve 22% success rates on average because the VLM has the commonsense knowledge of how to solve tasks, which can provide some reasonable information for the agents. Significantly, under the guidance of the foundation priors, FAC has an impressive average success rate of 86% across all the tasks.

Furthermore, the learned policy has the ability to adapt and refine its approach based on the prior policy, so as to successfully accomplish tasks, as exemplified in Fig. 5. Initially, the prior policy struggles with grasping the door handle, attempting to open the door without a successful grasp. In contrast, FAC persistently tries to secure the handle before pulling back the arm, which significantly

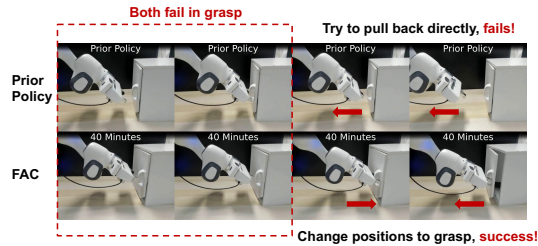


Figure 5: Prior policy attempts to open the door without a successful grasp, whereas FAC persistently tries to secure the handle before pulling back the arm through training.

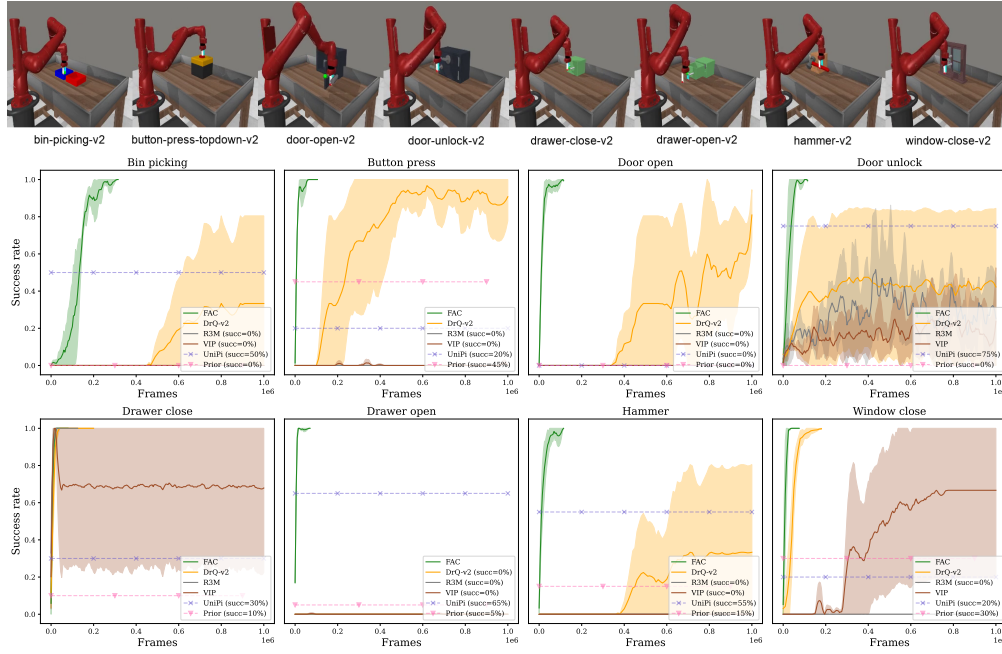


Figure 6: **Success Rate Curves for the 8 Tasks in Meta-World.** Our method consistently achieves **100% success rates** across all tasks, under the constrained performance of the policy prior model. It significantly outperforms the baselines with manual-designed rewards.

enhances performance. The remarkable performance of FAC proves the efficiency of our proposed framework. It indicates the substantial potential to leverage abundant prior knowledge for embodied agents under the RLFP framework.

4.2 Manipulation tasks in Simulations

Environments. We conduct experiments in 8 tasks from simulated robotics environment Meta-World [65], widely recognized for their ability to test diverse manipulation skills [60]. We average the success rates over 10 evaluation episodes across 3 runs with different seeds.

Acquiring Foundation Prior. (1) Prior success-reward. There are few foundation models to distinguish the success behavior in embodied AI, and we find that GPT-4V usually fails in simulation images. So we choose the ground-truth 0-1 success reward in simulation. We also distill a noisy success-reward model to ablate, in Sec. 4.3. (2) Prior policy. To demonstrate that the prior model can be agnostic to the forms, we choose diffusion foundation policy prior. We follow the pipeline of UniPi [25], which generates videos from diffusion models and infers actions from an inverse dynamics model. To make it more efficient, we offline distill a policy model by generating videos from diffusion models and inferred actions from the collected videos. We choose an open-sourced video diffusion model Seer [26], which predicts videos conditioned on images and language instructions. Ideally, the model can be plugged in without in-domain fine-tuning. However, we find the current open-source video prediction models fail to generate reasonable videos in the simulator. Consequently, we fine-tune the Seer with 10 example videos from each task. Compared to UniPi which fine-tunes with 200k videos, the videos generated by our model are much more noisy, attached in supplementary. (3) Prior value. We choose the model VIP [24], and keep the same usage as the experiments on real robots. Implementation details of the diffusion policy are in App. A.3.2.

Baselines. We benchmark our method against the following baselines: (1) Vanilla DrQ-v2 [11], with manually designed rewards from the suite; (2) R3M [46], VIP [24], where we integrate the DrQ-v2 with either the R3M or VIP visual representation backbones. These baselines also rely on manually designed rewards from the suite; (3) UniPi [25]; (4) The distilled policy from UniPi.

Performance Analysis in Meta-World. We compare the performance of our method with the above baselines on 8 tasks in Meta-World with 1M frames. Our proposed FAC achieves 100% success rates in all the tasks. 7/8 of them require fewer than 100k frames (about 1-hour training time). For the hard task bin-picking, FAC requires fewer than 400k frames. In contrast, the baseline methods can

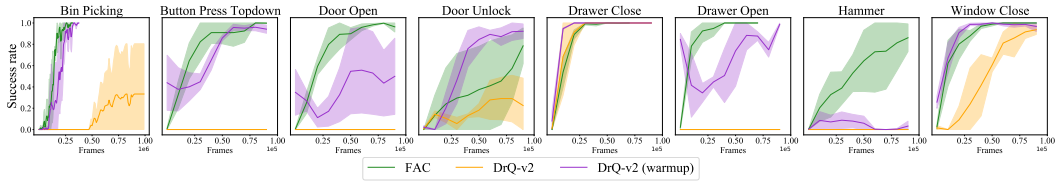


Figure 7: Comparison to the DrQ-v2 (warmup), which warm up the actor by 10 collected success demos from the prior policy model. FAC achieves better performance across the 8 tasks generally.

not achieve 100% success rates on most of tasks. As illustrated in Fig. 6, the sample efficiency and the success rates of FAC are much superior compared to the baseline methods. DrQ-v2 is able to complete some tasks but learns much slower compared to FAC. Moreover, we collect 10 success demos by the diffusion-based prior policy, and warm up the actor by the success demos before training. For the prior policy with 0 success rate, we collect 10 demos. The results are shown in Fig. 7. The improvement of DrQ-v2 with warmup by success demos is evident, but it still lags behind FAC generally. This is because FAC benefits from policy prior guidance during the training process.

R3M and VIP backbones inject the visual representation prior knowledge into the RL process, but their performance is even worse than DrQ-v2. We hypothesize that it might be caused by the pre-trained model having lost plasticity [66]. Since the UniPi and the distilled foundation prior policy do not involve interaction with the environments in training, they are represented as two horizontal lines in Fig. 6. UniPi outperforms the distilled prior in most environments, since the distilled prior is learned from UniPi. However, UniPi is still far inferior compared to FAC.

4.3 Ablation Study in Simulations

In this section, we answer the following questions: (I) What’s the importance of the three proposed priors? (II) How does FAC perform with noisier priors?

Ablation of Each Foundation Prior. To assess the significance of the three foundation prior, we conduct experiments by individually omitting each prior and comparing the results with the full method. Additionally, we included an ablation study focused on success trajectory imitation, a form of policy regularization. For convenience, we note the success buffer as the usage of success trajectory imitation in the result figure. Figure 8 (a) shows the four ablations.

We find that the reward prior is the most important, without which the performance over all the tasks drops a lot or even fails. The reason is that, without the 0-1 success signals, the reward function is reduced to the shaping reward, where any policy is equivalent under this reward. Without the policy prior, the agent fails on some hard tasks, such as bin-picking and door-open. It also converges much more slowly on most of tasks, such as door-unlock. Without the value prior or the success buffer, the sample efficiency would drop, especially for the hard task bin-picking. This is because, under noisy policy prior, the shaping rewards inferred from value prior can guide the policy towards states of higher values more effectively. Success trajectory imitation learns from successful trials, thereby enhancing sample efficiency. Generally, employing all foundation priors is the optimal strategy.

FAC with Various Quality of Foundation Priors. As shown in previous ablations, without value prior knowledge, the sample efficiency of FAC will drop by a degree. It indicates that a better value foundation prior can further boost performance. Here, we investigate how FAC is robust to the quality of the policy and success reward foundation priors. Firstly, we design several noisier policy priors. We discretize each action dimension generated from the distilled policy model into only three values $\{-1, 0, +1\}$. This makes the policy prior only contain rough directional information. We name this prior as *discretized policy*. To generate even noisier prior, we replace the discretized actions with uniform noise at 20% and 50% probability. As shown in Figure 8 (b1), we find that the discretized policy prior (in the blue curve) performs similarly to the original policy prior (in the green curve), except for bin-picking and door-unlock, which requires more frames to achieve 100% success rates. Adding extra noises decreases the performance further. However, even using the discretized policy with 50% noise, FAC can still reach 100% success rates in many environments. To further investigate the robustness, we apply systematically wrong policy prior, which has a 20% or 50% probability to make the prior action inverse (-1 changes to 1) in Figure 8 (b2). We find that FAC works well under the 20% ratio of the wrong direction, but the success rate drops a lot under the 50% ratio, which is full of misleading information. The results under the 20% ratio indicate that our method has good robustness to systematical noises.

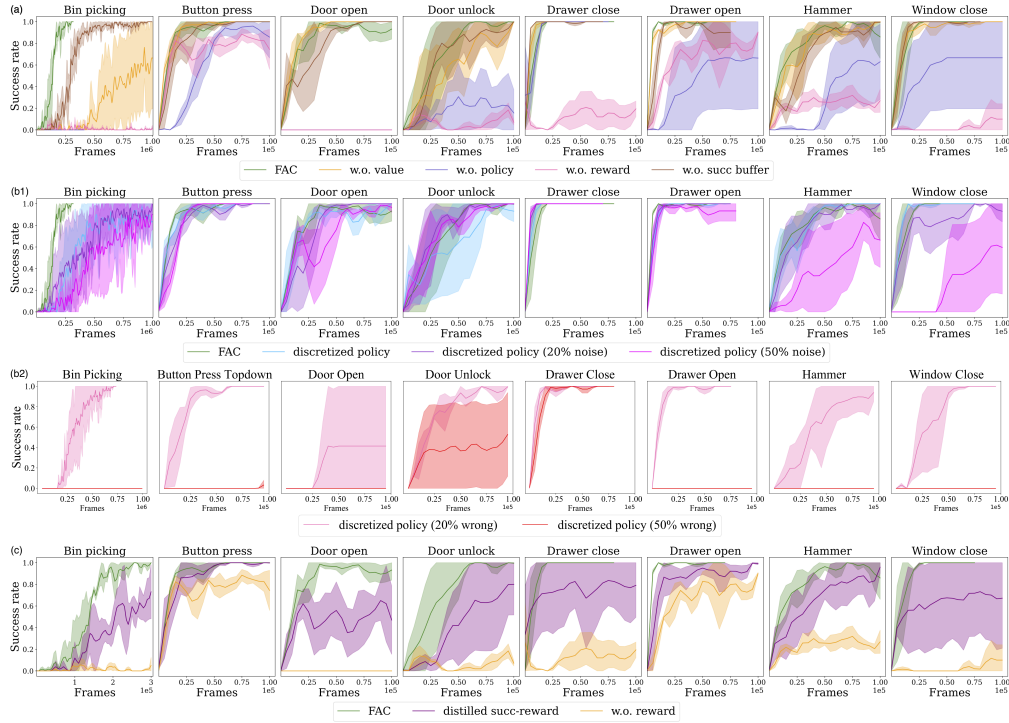


Figure 8: **Results of Ablation Study** (a) Three Foundation Priors and the Success Buffer. (b) The Quality of Policy Prior. (c) The Quality of the success-reward Prior.

Regarding the quality of the success-reward prior, we distill a proxy model with 50k offline data from the replay buffer, in total for all 8 tasks. The proxy model takes images as input and is conditioned on the task embeddings (multi-task), which has a 1.7% false positive error and 9.9% false negative error on the evaluation datasets. We replace the oracle 0-1 success reward with the predicted success reward. As depicted in Fig. 8 (c), compared to the oracle success-reward, FAC under the 50k-images-distilled model has a limited performance drop in the tasks generally. Moreover, it can achieve much superior performance than the FAC w.o. success reward. Consequently, the proposed FAC can work well under the noisy success-reward foundation prior. In summary, our ablation studies consistently demonstrate the resilience of FAC to variations in the quality of foundation priors. The higher the quality of the prior, the more sample-efficient FAC becomes.

5 Discussion

In this paper, we introduce a novel framework, termed Reinforcement Learning from Foundation Priors (RLFP), which leverages policy, value, and success-reward prior knowledge for RL. Additionally, we also detail the implementation of this concept within actor-critic methods, introducing the Foundation-guided Actor-Critic (FAC) approach. Extensive experiments on real robots and simulated environments demonstrate the effectiveness of our framework in enabling efficient autonomous learning by agents.

Limitation This work does have its limitations. It still relies on human engineering in designing the low-level skills and the prompts, such as providing the code policy demos and task descriptions. For the poor diffusion foundation models, we need to fine-tune with a few in-domain data to provide reasonable prior knowledge. However, as the performance of foundation models continues to improve, in the future, we may only need to provide very simple task instructions as prompts, without the need for fine-tuning the models.

Looking ahead, there are two dimensions for future exploration of this work. Firstly, it is imperative to construct accurate and broadly applicable foundation priors. Additionally, it is promising to introduce more abundant prior knowledge for the RLFP framework. For instance, humans can predict the future states. Such prediction prior knowledge can be extracted from the dynamic foundation models, which can be potentially more effective for policy learning.

References

- [1] J. Schrittwieser, I. Antonoglou, T. Hubert, K. Simonyan, L. Sifre, S. Schmitt, A. Guez, E. Lockhart, D. Hassabis, T. Graepel, et al. Mastering atari, go, chess and shogi by planning with a learned model. *Nature*, 588(7839):604–609, 2020.
- [2] W. Ye, S. Liu, T. Kurutach, P. Abbeel, and Y. Gao. Mastering atari games with limited data. *Advances in Neural Information Processing Systems*, 34:25476–25488, 2021.
- [3] K. Arulkumaran, A. Cully, and J. Togelius. Alphastar: An evolutionary computation perspective. In *Proceedings of the genetic and evolutionary computation conference companion*, pages 314–315, 2019.
- [4] D. Yarats, R. Fergus, A. Lazaric, and L. Pinto. Mastering visual continuous control: Improved data-augmented reinforcement learning. *arXiv preprint arXiv:2107.09645*, 2021.
- [5] A. G. Barto, R. S. Sutton, and C. W. Anderson. Neuronlike adaptive elements that can solve difficult learning control problems. *IEEE transactions on systems, man, and cybernetics*, (5): 834–846, 1983.
- [6] S. Mahadevan and J. Connell. Automatic programming of behavior-based robots using reinforcement learning. *Artificial intelligence*, 55(2-3):311–365, 1992.
- [7] P. Wu, A. Escontrela, D. Hafner, P. Abbeel, and K. Goldberg. Daydreamer: World models for physical robot learning. In *Conference on Robot Learning*, pages 2226–2240. PMLR, 2023.
- [8] J. Yang, M. S. Mark, B. Vu, A. Sharma, J. Bohg, and C. Finn. Robot fine-tuning made easy: Pre-training rewards and policies for autonomous real-world reinforcement learning. *arXiv preprint arXiv:2310.15145*, 2023.
- [9] S. Haldar, J. Pari, A. Rai, and L. Pinto. Teach a robot to fish: Versatile imitation from one minute of demonstrations. *arXiv preprint arXiv:2303.01497*, 2023.
- [10] D. Silver, T. Hubert, J. Schrittwieser, I. Antonoglou, M. Lai, A. Guez, M. Lanctot, L. Sifre, D. Kumaran, T. Graepel, et al. Mastering chess and shogi by self-play with a general reinforcement learning algorithm. *arXiv preprint arXiv:1712.01815*, 2017.
- [11] D. Yarats, R. Fergus, A. Lazaric, and L. Pinto. Mastering visual continuous control: Improved data-augmented reinforcement learning. *arXiv preprint arXiv:2107.09645*, 2021.
- [12] D. Hafner, J. Pasukonis, J. Ba, and T. Lillicrap. Mastering diverse domains through world models. *arXiv preprint arXiv:2301.04104*, 2023.
- [13] N. Hansen, H. Su, and X. Wang. Td-mpc2: Scalable, robust world models for continuous control. *arXiv preprint arXiv:2310.16828*, 2023.
- [14] A. N. Meltzoff. Infant imitation after a 1-week delay: long-term memory for novel acts and multiple stimuli. *Developmental psychology*, 24(4):470, 1988.
- [15] A. N. Meltzoff. Understanding the intentions of others: re-enactment of intended acts by 18-month-old children. *Developmental psychology*, 31(5):838, 1995.
- [16] A. Vaswani, N. Shazeer, N. Parmar, J. Uszkoreit, L. Jones, A. N. Gomez, Ł. Kaiser, and I. Polosukhin. Attention is all you need. *Advances in neural information processing systems*, 30, 2017.
- [17] J. Devlin, M.-W. Chang, K. Lee, and K. Toutanova. Bert: Pre-training of deep bidirectional transformers for language understanding. *arXiv preprint arXiv:1810.04805*, 2018.

- [18] T. Brown, B. Mann, N. Ryder, M. Subbiah, J. D. Kaplan, P. Dhariwal, A. Neelakantan, P. Shyam, G. Sastry, A. Askell, et al. Language models are few-shot learners. *Advances in neural information processing systems*, 33:1877–1901, 2020.
- [19] OpenAI. GPT-4 technical report. *CoRR*, abs/2303.08774, 2023. doi:10.48550/arXiv.2303.08774. URL <https://doi.org/10.48550/arXiv.2303.08774>.
- [20] A. Dosovitskiy, L. Beyer, A. Kolesnikov, D. Weissenborn, X. Zhai, T. Unterthiner, M. Dehghani, M. Minderer, G. Heigold, S. Gelly, et al. An image is worth 16x16 words: Transformers for image recognition at scale. *arXiv preprint arXiv:2010.11929*, 2020.
- [21] A. Radford, J. W. Kim, C. Hallacy, A. Ramesh, G. Goh, S. Agarwal, G. Sastry, A. Askell, P. Mishkin, J. Clark, et al. Learning transferable visual models from natural language supervision. In *International conference on machine learning*, pages 8748–8763. PMLR, 2021.
- [22] A. Ramesh, P. Dhariwal, A. Nichol, C. Chu, and M. Chen. Hierarchical text-conditional image generation with clip latents. *arXiv preprint arXiv:2204.06125*, 2022.
- [23] A. Kirillov, E. Mintun, N. Ravi, H. Mao, C. Rolland, L. Gustafson, T. Xiao, S. Whitehead, A. C. Berg, W.-Y. Lo, et al. Segment anything. *arXiv preprint arXiv:2304.02643*, 2023.
- [24] Y. J. Ma, S. Sodhani, D. Jayaraman, O. Bastani, V. Kumar, and A. Zhang. Vip: Towards universal visual reward and representation via value-implicit pre-training. *arXiv preprint arXiv:2210.00030*, 2022.
- [25] Y. Du, M. Yang, B. Dai, H. Dai, O. Nachum, J. Tenenbaum, D. Schuurmans, and P. Abbeel. Learning universal policies via text-guided video generation. *arXiv preprint arXiv:2302.00111*, 2023.
- [26] X. Gu, C. Wen, J. Song, and Y. Gao. Seer: Language instructed video prediction with latent diffusion models. *arXiv preprint arXiv:2303.14897*, 2023.
- [27] A. Brohan, N. Brown, J. Carbajal, Y. Chebotar, J. Dabis, C. Finn, K. Gopalakrishnan, K. Hausman, A. Herzog, J. Hsu, et al. Rt-1: Robotics transformer for real-world control at scale. *arXiv preprint arXiv:2212.06817*, 2022.
- [28] A. Brohan, N. Brown, J. Carbajal, Y. Chebotar, X. Chen, K. Choromanski, T. Ding, D. Driess, A. Dubey, C. Finn, et al. Rt-2: Vision-language-action models transfer web knowledge to robotic control. *arXiv preprint arXiv:2307.15818*, 2023.
- [29] S. Reed, K. Zolna, E. Parisotto, S. G. Colmenarejo, A. Novikov, G. Barth-Maron, M. Gimenez, Y. Sulsky, J. Kay, J. T. Springenberg, et al. A generalist agent. *arXiv preprint arXiv:2205.06175*, 2022.
- [30] T. Yu, T. Xiao, A. Stone, J. Tompson, A. Brohan, S. Wang, J. Singh, C. Tan, J. Peralta, B. Ichter, et al. Scaling robot learning with semantically imagined experience. *arXiv preprint arXiv:2302.11550*, 2023.
- [31] Y. Chebotar, K. Hausman, F. Xia, Y. Lu, A. Irpan, A. Kumar, T. Yu, A. Herzog, K. Pertsch, K. Gopalakrishnan, et al. Q-transformer: Scalable offline reinforcement learning via autoregressive q-functions. In *7th Annual Conference on Robot Learning*, 2023.
- [32] N. Di Palo, A. Byravan, L. Hasenclever, M. Wulfmeier, N. Heess, and M. Riedmiller. Towards a unified agent with foundation models. In *Workshop on Reincarnating Reinforcement Learning at ICLR 2023*.
- [33] W. Huang, F. Xia, T. Xiao, H. Chan, J. Liang, P. Florence, A. Zeng, J. Tompson, I. Mordatch, Y. Chebotar, et al. Inner monologue: Embodied reasoning through planning with language models. *arXiv preprint arXiv:2207.05608*, 2022.

- [34] M. Ahn, A. Brohan, N. Brown, Y. Chebotar, O. Cortes, B. David, C. Finn, K. Gopalakrishnan, K. Hausman, A. Herzog, et al. Do as i can, not as i say: Grounding language in robotic affordances. *arXiv preprint arXiv:2204.01691*, 2022.
- [35] D. Driess, F. Xia, M. S. Sajjadi, C. Lynch, A. Chowdhery, B. Ichter, A. Wahid, J. Tompson, Q. Vuong, T. Yu, et al. Palm-e: An embodied multimodal language model. *arXiv preprint arXiv:2303.03378*, 2023.
- [36] J. Wu, R. Antonova, A. Kan, M. Lepert, A. Zeng, S. Song, J. Bohg, S. Rusinkiewicz, and T. Funkhouser. Tidybot: Personalized robot assistance with large language models. *arXiv preprint arXiv:2305.05658*, 2023.
- [37] I. Singh, V. Blukis, A. Mousavian, A. Goyal, D. Xu, J. Tremblay, D. Fox, J. Thomason, and A. Garg. Progprompt: Generating situated robot task plans using large language models. In *2023 IEEE International Conference on Robotics and Automation (ICRA)*, pages 11523–11530. IEEE, 2023.
- [38] M. Shridhar, L. Manuelli, and D. Fox. Cliport: What and where pathways for robotic manipulation. In *Conference on Robot Learning*, pages 894–906. PMLR, 2022.
- [39] Y. Hu, F. Lin, T. Zhang, L. Yi, and Y. Gao. Look before you leap: Unveiling the power of gpt-4v in robotic vision-language planning. *arXiv preprint arXiv:2311.17842*, 2023.
- [40] J. Liang, W. Huang, F. Xia, P. Xu, K. Hausman, B. Ichter, P. Florence, and A. Zeng. Code as policies: Language model programs for embodied control. In *2023 IEEE International Conference on Robotics and Automation (ICRA)*, pages 9493–9500. IEEE, 2023.
- [41] W. Huang, C. Wang, R. Zhang, Y. Li, J. Wu, and L. Fei-Fei. Voxposer: Composable 3d value maps for robotic manipulation with language models. *arXiv preprint arXiv:2307.05973*, 2023.
- [42] J. Ho, W. Chan, C. Saharia, J. Whang, R. Gao, A. Gritsenko, D. P. Kingma, B. Poole, M. Norouzi, D. J. Fleet, and T. Salimans. Imagen video: High definition video generation with diffusion models, 2022.
- [43] S. Karamcheti, S. Nair, A. S. Chen, T. Kollar, C. Finn, D. Sadigh, and P. Liang. Language-driven representation learning for robotics. *arXiv preprint arXiv:2302.12766*, 2023.
- [44] R. Shah and V. Kumar. Rrl: Resnet as representation for reinforcement learning. *arXiv preprint arXiv:2107.03380*, 2021.
- [45] A. Majumdar, K. Yadav, S. Arnaud, Y. J. Ma, C. Chen, S. Silwal, A. Jain, V.-P. Berges, P. Abbeel, J. Malik, et al. Where are we in the search for an artificial visual cortex for embodied intelligence? *arXiv preprint arXiv:2303.18240*, 2023.
- [46] S. Nair, A. Rajeswaran, V. Kumar, C. Finn, and A. Gupta. R3m: A universal visual representation for robot manipulation. *arXiv preprint arXiv:2203.12601*, 2022.
- [47] M. Shridhar, L. Manuelli, and D. Fox. Perceiver-actor: A multi-task transformer for robotic manipulation. In *Conference on Robot Learning*, pages 785–799. PMLR, 2023.
- [48] S. Nair, E. Mitchell, K. Chen, S. Savarese, C. Finn, et al. Learning language-conditioned robot behavior from offline data and crowd-sourced annotation. In *Conference on Robot Learning*, pages 1303–1315. PMLR, 2022.
- [49] Y. Jiang, A. Gupta, Z. Zhang, G. Wang, Y. Dou, Y. Chen, L. Fei-Fei, A. Anandkumar, Y. Zhu, and L. Fan. Vima: General robot manipulation with multimodal prompts. *arXiv preprint arXiv:2210.03094*, 2022.

- [50] L. Fan, G. Wang, Y. Jiang, A. Mandlekar, Y. Yang, H. Zhu, A. Tang, D.-A. Huang, Y. Zhu, and A. Anandkumar. Minedojo: Building open-ended embodied agents with internet-scale knowledge. *arXiv preprint arXiv:2206.08853*, 2022.
- [51] S. Nair, E. Mitchell, K. Chen, S. Savarese, C. Finn, et al. Learning language-conditioned robot behavior from offline data and crowd-sourced annotation. In *Conference on Robot Learning*, pages 1303–1315. PMLR, 2022.
- [52] P. Mahmoudieh, D. Pathak, and T. Darrell. Zero-shot reward specification via grounded natural language. In *International Conference on Machine Learning*, pages 14743–14752. PMLR, 2022.
- [53] C. Eteke, D. Kebüde, and B. Akgün. Reward learning from very few demonstrations. *IEEE Transactions on Robotics*, 37(3):893–904, 2020.
- [54] B. Wu, F. Xu, Z. He, A. Gupta, and P. K. Allen. Squirrel: Robust and efficient learning from video demonstration of long-horizon robotic manipulation tasks. In *2020 IEEE/RSJ International Conference on Intelligent Robots and Systems (IROS)*, pages 9720–9727. IEEE, 2020.
- [55] H. Xiong, R. Mendonca, K. Shaw, and D. Pathak. Adaptive mobile manipulation for articulated objects in the open world. *arXiv preprint arXiv:2401.14403*, 2024.
- [56] I. Popov, N. Heess, T. Lillicrap, R. Hafner, G. Barth-Maron, M. Vecerik, T. Lampe, Y. Tassa, T. Erez, and M. Riedmiller. Data-efficient deep reinforcement learning for dexterous manipulation. *arXiv preprint arXiv:1704.03073*, 2017.
- [57] W. Ye, Y. Zhang, P. Abbeel, and Y. Gao. Become a proficient player with limited data through watching pure videos. In *The Eleventh International Conference on Learning Representations*, 2022.
- [58] S. Wang, S. Liu, W. Ye, J. You, and Y. Gao. Efficientzero v2: Mastering discrete and continuous control with limited data. *arXiv preprint arXiv:2403.00564*, 2024.
- [59] D. Hafner, J. Pasukonis, J. Ba, and T. Lillicrap. Mastering diverse domains through world models. *arXiv preprint arXiv:2301.04104*, 2023.
- [60] S. Haldar, V. Mathur, D. Yarats, and L. Pinto. Watch and match: Supercharging imitation with regularized optimal transport. In *Conference on Robot Learning*, pages 32–43. PMLR, 2023.
- [61] P. Lancaster, N. Hansen, A. Rajeswaran, and V. Kumar. Modem-v2: Visuo-motor world models for real-world robot manipulation. *arXiv preprint arXiv:2309.14236*, 2023.
- [62] A. Y. Ng, D. Harada, and S. Russell. Policy invariance under reward transformations: Theory and application to reward shaping. In *Icml*, volume 99, pages 278–287. Citeseer, 1999.
- [63] S. Fujimoto, H. Hoof, and D. Meger. Addressing function approximation error in actor-critic methods. In *International conference on machine learning*, pages 1587–1596. PMLR, 2018.
- [64] P. J. Ball, L. Smith, I. Kostrikov, and S. Levine. Efficient online reinforcement learning with offline data. *arXiv preprint arXiv:2302.02948*, 2023.
- [65] T. Yu, D. Quillen, Z. He, R. Julian, K. Hausman, C. Finn, and S. Levine. Meta-world: A benchmark and evaluation for multi-task and meta reinforcement learning. In *Conference on robot learning*, pages 1094–1100. PMLR, 2020.
- [66] P. D’Oro, M. Schwarzer, E. Nikishin, P.-L. Bacon, M. G. Bellemare, and A. Courville. Sample-efficient reinforcement learning by breaking the replay ratio barrier. In *Deep Reinforcement Learning Workshop NeurIPS 2022*, 2022.

- [67] M. Dorigo and M. Colombetti. *Robot shaping: an experiment in behavior engineering*. MIT press, 1998.
- [68] M. J. Mataric. Reward functions for accelerated learning. In *Machine learning proceedings 1994*, pages 181–189. Elsevier, 1994.
- [69] J. Randløv and P. Alstrøm. Learning to drive a bicycle using reinforcement learning and shaping. In *ICML*, volume 98, pages 463–471, 1998.
- [70] E. Cetin, P. J. Ball, S. Roberts, and O. Celiktutan. Stabilizing off-policy deep reinforcement learning from pixels. *arXiv preprint arXiv:2207.00986*, 2022.
- [71] R. Zheng, X. Wang, Y. Sun, S. Ma, J. Zhao, H. Xu, H. Daumé III, and F. Huang. Taco: Temporal latent action-driven contrastive loss for visual reinforcement learning. *arXiv preprint arXiv:2306.13229*, 2023.
- [72] R. Cheng, A. Verma, G. Orosz, S. Chaudhuri, Y. Yue, and J. Burdick. Control regularization for reduced variance reinforcement learning. In *International Conference on Machine Learning*, pages 1141–1150. PMLR, 2019.

A Appendix

Appendix Table of Contents

- Appendix A.1: Reward Shaping in FAC
- Appendix A.2: Experimental Details of FAC
- Appendix A.3: Details of Acquiring Foundation Priors
- Appendix A.4: Running Clock Time Analysis
- Appendix A.5: More Ablations Results
- Appendix A.6: Proof of the Optimality under Policy Regularization

A.1 Reward Shaping in FAC

In this work, we apply the value prior knowledge in Actor-Critic algorithms in the format of reward shaping. Reward shaping guides the RL process of an agent by supplying additional rewards for the MDP [67, 68, 69]. In practice, it is considered a promising method to speed up the learning process for complex problems. Ng et al. [62] introduce a formal framework for designing shaping rewards. Specifically, we define the MDP $\mathcal{G} = (\mathcal{S}, \mathcal{A}, \mathcal{P}, \mathcal{R})$, where \mathcal{A} denotes the action space, and $\mathcal{P} = \Pr\{s_{t+1}|s_t, a_t\}$ denotes the transition probabilities. Rather than handling the MDP \mathcal{G} , the agent learns policies on some transformed MDP $\mathcal{G}' = (\mathcal{S}, \mathcal{A}, \mathcal{P}, \mathcal{R}')$, $\mathcal{R}' = \mathcal{R} + F$, where F is the shaping reward function. When there exists a state-only function $\Phi : \mathcal{S} \rightarrow \mathbb{R}^1$ such that $F(s, a, s') = \gamma\Phi(s') - \Phi(s)$ (γ is the discounting factor), the F is called a **potential-based shaping function**. Ng et al. [62] prove that the potential-based shaping function F has optimal policy consistency under some conditions as follows:

Theorem 1 [62] *Suppose that F takes the form of $F(s, a, s') = \gamma\Phi(s') - \Phi(s)$, $\Phi(s_0) = 0$ if $\gamma = 1$, then for $\forall s \in \mathcal{S}, a \in \mathcal{A}$, the potential-based F preserve optimal policies and we have:*

$$\begin{aligned} Q_{\mathcal{G}'}^*(s, a) &= Q_{\mathcal{G}}^*(s, a) - \Phi(s) \\ V_{\mathcal{G}'}^*(s) &= V_{\mathcal{G}}^*(s) - \Phi(s) \end{aligned} \quad (2)$$

The theorem indicates that the potential-based shaping rewards treat every policy equally. Thus it does not prefer $\pi_{\mathcal{G}}^*$. Moreover, under the guidance of shaping rewards for the agents, a significant reduction in learning time can be achieved. In practical settings, the real-valued function Φ can be determined based on domain knowledge.

A.2 Experimental Details of FAC

Since FAC is built upon DrQ-v2, the hyper-parameters of training the actor-critic model are the same as DrQ-v2 [11]. The n-step TD target value and the action in Eq. 1 are as follows, where $\bar{\theta}_k$ are the moving weights for Q target networks.

$$\begin{aligned} y &= \sum_{i=0}^{n-1} \gamma^i r_{t+i} + \gamma^n \min_{k=1,2} Q_{\bar{\theta}_k}(s_{t+n}, a_{t+n}), \\ a_t &= \pi_{\phi}(s_t) + \epsilon, \epsilon \sim \text{clip}(\mathcal{N}(0, \sigma^2), -c, c) \end{aligned} \quad (3)$$

Hyper-parameters in FAC Moreover, the observation shape is 84×84 on real robots and in simulation. For better representations of the scene, we use a wrist camera on real robots. In simulation, we stack 3 frames and repeat actions for 2 steps, while we do not stack frames or repeat actions on real robots. In Meta-World, we follow the experimental setup of [60]. Specifically, the horizon length is set to 125 frames for all tasks except for bin-picking and button-press-topdown, which are set to 175. The total frames of the 8 tasks are 100k, except for the task bin-picking, which is set to 1M. Notably, we set the same camera view of all the tasks for consistency. On real robots, we set the

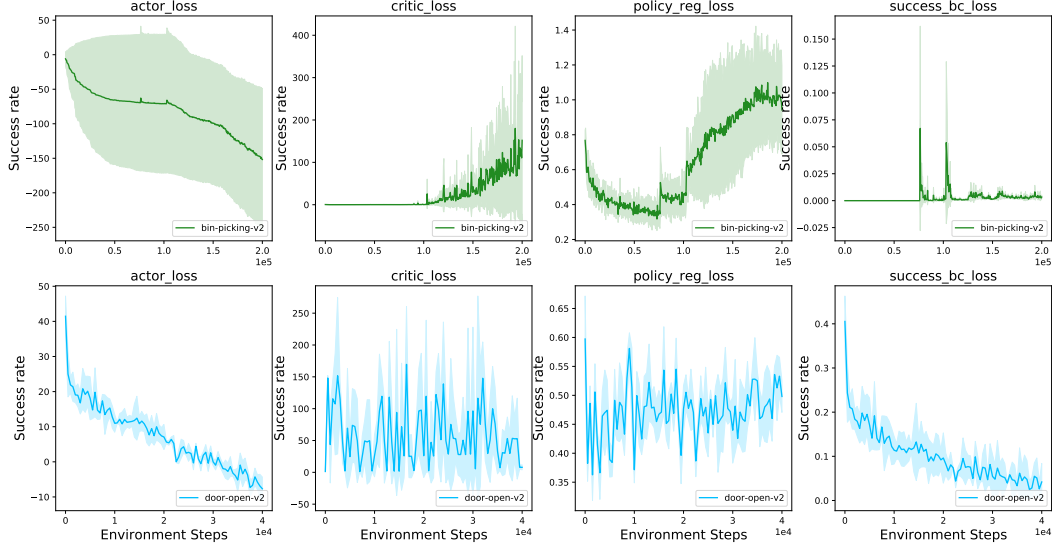


Figure 9: Training loss curves of bin-picking and door-open.

horizon of the 5 tasks (Pick Place, Open Door, Water Plants, Unscrew Bottle Cap, Play Golf) to 40, 40, 50, 60, and 25, respectively. We evaluate them every 10 minutes, and the positions of the objects vary in 5cm in Pick Place, Open Door, Watering Plants, and 3cm in Unscrew Bottle Cap and Play Golf. We reset the objects manually because the current foundation model cannot deal with reset problems. The difference in the hyper-parameters between the real robots and the simulation is as follows:

Table 2: The Main Difference of the Hyper-parameters of FAC on real robots and in simulation.

Parameter	On real robots	In simulation
Frame Stack	1	3
Action Repeat	1	2
Seed Frames	10 Trajectory	4000
Std of Actor	0.1	1 \rightarrow 0.1
Feature_dim in DrQ-v2	512	50
UTD ratio	20	1 (N/A)
Choose better action under Q	Yes	No
Use wrist camera	Yes	No

The training loss curves of the task bin-picking and door-open for reference, as shown in Fig. 9.

More Experimental Setup Details on real robots

Here we give the task description of the 5 tasks on Franka Arm. For the task Unscrew Bottle Cap, we will fix the bottle when the arm tries to unscrew the cap.

- Pick Place: *Pick up the purple eggplant and place it onto the blue plate.*
- Open Door: *There is a white cabinet on the table and there is a cucumber in it. The door can only be opened from the outside. Please open the door by a large margin so that the cucumber can be seen.*
- Watering Plants: *There are a blue watering kettle and a potted plant. Please help me watering the plant and keep watering still.*
- Unscrew Bottle Cap: *There are a plastic bottle with a green cap and a pink plate on the table. The bottle will be fixed on the table, so that you cannot lift the bottle. Please help me*

unscrew the bottle cap and place it on the pink plate. You must know how to unscrew the bottle cap, anticlockwise or clockwise?

- Play Golf: *There is a golf hole and a golf ball on the table. The robotic arm is tied by a golf club. Please shoot the golf ball into the set.*

The ground-truth success reward functions of each task are as follows, which is leveraged in evaluation.

- Pick Place: $\text{dist}(\text{xy position of the eggplant}, \text{xy position of the blue plate center}) < \text{radius}$ & $\text{dist}(z \text{ of the eggplant}, z \text{ of the blue plate}) < \epsilon$, $\epsilon = 0.01$.
- Open Door: $\text{dist}(\text{xy position of the handle}, \text{xy position of the cabinet center}) > \epsilon$, $\epsilon = 0.1$.
- Watering Plants: $\text{dist}(z \text{ of the sprout}, z \text{ of the plants}) > \epsilon_1$ & $\text{dist}(\text{xy of the sprout}, \text{xy of the plants}) < \text{radius}$ & $\text{abs}(\text{horizontal orientation of the sprout}) < \epsilon_2 \text{ degree}$, $\epsilon_1 = 0.1$, $\epsilon_2 = 15$.
- Unscrew Bottle Cap: $\text{dist}(\text{xyz of the cap}, \text{xyz of the bottle center}) > \epsilon$ & $(\text{cap in the plate})$, $\epsilon = 0.15$. ('cap in the plate' is the same as the function in pick place).
- Play Golf: $(\text{golf in the golf hole})$. ('golf in the golf hole' is the same as the function in pick place).

Reward functions for vanilla RL Since it is hard to get the object state in real time, we assume the object state will be attached to the robot state after some actions. For example, we have the initial position of the eggplant, the position, and the size of the target plate. After the gripper reaches the pos of the eggplant and takes action "grasp", the pos of the eggplant will be set the same as the eef pos. The reward function is the normal pick-place reward function. For the door-open, we get the handle initial position, and once the arm is reaching in the bound of 5cm of the handle and closes the gripper, the position of the handle will be attached to the eef of the robot. Therefore, the reward functions are based on the distance between the gripper and some target position sequences, including the position distance and the orientation distance. We give the reward functions of the Door Open and Play Golf as examples, which are harder tasks.

Open Door: $R_{\text{approach}} = \max(0, 1 - \tanh(10 \times \|\mathbf{p}_{\text{gripper}} - \mathbf{p}_{\text{handle}}\|))$, encourages the robot to get closer to the handle by diminishing rewards as the distance decreases. $R_{\text{orient}} = 1 - \frac{\|\mathbf{q}_{\text{gripper}} - \mathbf{q}_{\text{handle}}\|}{2}$, incentivizes aligning the robot's gripper orientation with that of the handle. $R_{\text{pull}} = \max(0, \theta_{\text{door}} - \theta_{\text{prev_door}})$, increases with the door's opening angle. $R_{\text{open}} = \min(\frac{\theta_{\text{door}}}{90.0}, 1.0)$, prioritizes achieving a 90-degree opening. A small time penalty, $R_{\text{time}} = -0.01$, is applied per time step to encourage faster task completion. The total reward is then formulated as: $R_{\text{total}} = 0.01 * R_{\text{approach}} + 0.05 * R_{\text{orient}} + 0.1 * R_{\text{pull}} + 0.1 * R_{\text{open}} + R_{\text{time}}$.

Play Golf: We use the golf club's length and the end-effector's (eef) position to determine the clubhead's state. The ball back position is defined as the back of the ball, which is the optimal point to strike. $R_{\text{approach}} = \max(0, 1 - \tanh(10 \times \|\mathbf{p}_{\text{clubhead}} - \mathbf{p}_{\text{ball_back}}\|))$, encourages the robot to position the clubhead at the back of the ball. $R_{\text{orient}} = 1 - \frac{\|\mathbf{q}_{\text{clubhead}} - \mathbf{q}_{\text{target}}\|}{2}$, which incentivizes proper alignment of the clubhead for an accurate strike. Additionally, the reward for the clubhead's velocity at the moment of impact, $R_{\text{velocity}} = \max(0, 1 - \tanh(10 \times \|\mathbf{v}_{\text{clubhead}} - \mathbf{v}_{\text{desired}}\|))$, ensures that the clubhead reaches the optimal speed to strike the ball effectively. So the final reward is: $R_{\text{total}} = 0.1 * R_{\text{approach}} + 0.5 * R_{\text{orient}} + 0.5 * R_{\text{velocity}} + R_{\text{time}}$.



1 The robotic arm in the image appears to have positioned the spout of the watering can directly over the plant, which suggests that it is in the process of watering the plant. This setup is typically indicative of an automated or robotic system designed to water plants without human intervention.

0 The spout of the watering can is not oriented horizontally over the plant; rather, it is tilted at an angle that suggests it may not be actively watering the plant at this moment. It appears to be in a position that might be before or after the watering action, or possibly in a paused state.

Figure 10: Example of success identification by GPT-4V in task Watering Plants. Given the question. *Does the robotic arm water the plants? Attention, if the spout orients horizontally over the plant, you should output 1 for yes. Otherwise, you should output 0 for no without any space first. Be sure of your answer and explain your reason afterward.* The foundation model can give the correct success reward as well as the corresponding explanations.

A.3 Details of Acquiring Foundation Priors

A.3.1 Acquiring Foundation Priors on Franka

Examples of Success-reward Discrimination Prompts It is significant to feed the success-reward model by high-resolution images, which we choose 512×512 . Here we give an example of the success-reward prompts in FAC towards the task Watering Plants, by leveraging GPT-4V, as follows: *Does the robotic arm water the plants? Attention, if the spout orients over horizontally over the plant, you should output 1 for yes. Otherwise, you should output 0 for no without any space first. Be sure of your answer and explain your reason afterward.* Then we can receive the corresponding success-reward as well as the explanations, shown in Fig. 10.

Examples of Code Policy Prompts. Before code generation, we define some primitive skills. We implement the corresponding interface between primitive skills and control systems, so that they can be executed directly by the robot. The primitive low-level skills and the corresponding params are as follows:

- move_to x y z: move the gripper to the position (x, y, z).
- grasp: grasp with the gripper.
- release: release the gripper.
- rotate_clockwise: rotate gripper clockwise by 90 degree.
- rotate_anticlockwise: rotate gripper anticlockwise by 90 degree.
- orient_half_horizontally: change the orientation of the gripper half horizontally to make it grasp more easily.
- orient_vertically: change the orientation of the gripper vertically to make ti grasp something vertically.
- strike_front: strike something to the front of the arm.
- strick_back: strike something to the back of the arm.

Firstly, we input prompts that include a task description, the initial scene, and the expected format for the generated code. Notably, the task used in the example differs from the five tasks we evaluate. For

the downstream tasks, we rely on the GPT-4V to generate the code policy based on new images and the corresponding task descriptions, shown in Fig. 11. We also specify the range of object positions within the scene, enabling the VLM to estimate the position of the target object and generate code that includes skill plans and position parameters. Limited to the current ability of GPT-4V, it can build reasonable code policies under small changes in object positions.

Then, we feed in the current image and the task descriptions: *There are a plastic bottle with a green cap and a pink plate on the table. The bottle will be fixed on the table, so that you cannot lift the bottle. Please help me unscrew the bottle cap and place it on the pink plate. You must know how to unscrew the bottle cap, anticlockwise or clockwise?* Then we can receive the **generated code policy** as shown in the code text, which can make the correct rotation to unscrew the cap.

On real robots, the action space is 7-dim, consisting of the delta position (x, y, z) of the gripper, the delta orientation (roll yaw pitch) of the gripper, and the grasp/release of the gripper. We use the OSC control mode. As for the policy output of the code policy, it generates plans like “move_to $x_1 y_1 z_1$ ”. Then we use robotics control toolkits to compute the delta position/orientation for the robot, which is the prior action. Once the plan “move_to $x_1 y_1 z_1$ ” is finished (close to epsilon in practice), the code policy will execute the next plan. In this way, we can acquire the corresponding prior action in each step. The KL constraint is between the prior action and the RL policy. Consequently, the GPT-4V generates code plans that consist of the primitive skills, and then the primitive skill can generate delta prior actions by robotics control codes.



Figure 11: Initial observation image of the task Unscrew Bottle Cap, including the fixed camera view and the wrist camera view.

Policy Description Prompts for Unscrew Bottle Cap

```
# Query: pick up the plastic bottle
# Some info... (skip here)
# Here are the skills that you can choose:
# 1. move_to x y z: move the gripper to
#    the position of (x, y, z)
# 2. grasp: grasp with the gripper
# 3. release: release the gripper
# 4. rotate_clockwise: rotate the gripper
#    clockwise by only 90 degree
# 5. rotate_anticlockwise: rotate the
#    gripper anticlockwise by 90 degree
# 6. reset: move back to the initial
#    position
# Attention: For safety, you cannot rotate
#    clockwise or rotate
#    anticlockwise twice continuously. Think
#    carefully about how to
#    finish the task.

def code_policy():
    # Obtain the position of plastic
    #    bottle. Estimate the position.
    object_pos = [0.5, 0., 0.12]
    x1, y1, z1 = object_pos
    # Pick up
    plans = [
        # move above the bottle
        f'move_to {x1:.2f} {y1:.2f} {z1 +
        0.05:.2f}',
        # move to the bottle
        f'move_to {x1:.2f} {y1:.2f} {z1:.2
        f}',
        # grasp the bottle
        'grasp',
        # lift the cucumber
        f'move_to {x1:.2f} {y1:.2f} {z1 +
        0.2:.2f}',
    ]
    return plans
```

Generated Code Policy for Unscrew Bottle Cap

```
def code_policy():
    # Bottle cap position (estimated near
    #    the top of the bottle: height of
    #    the bottle + table z-axis)
    cap_pos = [0.5, 0., 0.26]
    x1, y1, z1 = cap_pos

    # Plate position (estimated to be at
    #    the provided position)
    plate_pos = [0.75, 0., 0.06]
    x2, y2, z2 = plate_pos

    # Plans to unscrew the bottle cap and
    #    place it on the plate
    plans = [
        # Move above the bottle cap
        f'move_to {x1:.2f} {y1:.2f} {z1 +
        0.05:.2f}',
        # Move to the bottle cap
        f'move_to {x1:.2f} {y1:.2f} {z1:.2
        f}',
        # Grasp the bottle cap
        f'grasp',
        # Rotate anticlockwise to unscrew
        f'rotate_anticlockwise',
        # Lift the cap
        f'move_to {x1:.2f} {y1:.2f} {z1 +
        0.05:.2f}',
        # Move above the plate
        f'move_to {x2:.2f} {y2:.2f} {z1 +
        0.05:.2f}',
        # Move down to the plate
        f'move_to {x2:.2f} {y2:.2f} {z2:.2
        f}',
        # Release the cap onto the plate
        f'release',
        # Move away
        f'move_to {x2:.2f} {y2:.2f} {z2 +
        0.2:.2f}'
    ]
    return plans
# done
```

A.3.2 Acquiring Foundation Priors on Meta-world

Training Inverse Dynamics Model We build the inverse dynamics model $\rho(s_t, s_{t+1})$ as follows:

- Takes inputs as s_t, s_{t+1} , with the shape of $3 \times 84 \times 84$.
- A Downsample Model, which outputs the representation with the shape of $128 \times 2 \times 2$.
- Flatten the planes into 512-dimension vectors.
- 1 Linear layer with ReLU, which outputs the 64-dimension vectors.
- 1 Linear layer with ReLU, which outputs the 64-dimension vectors.
- 1 Linear layer with ReLU, which outputs the action dimension vectors (equal to 4).

The Downsample model is designed as follows:

- 1 convolution with stride 2 and 128 output planes, output resolution 42×42 . (ReLU)
- 2 residual block with 128 planes.
- Average pooling with stride 2 (kernel size is 3), output resolution 21×21 . (ReLU)
- 2 residual block with 128 planes.
- Average pooling with stride 3 (kernel size is 5), output resolution 7×7 . (ReLU)
- 2 residual block with 128 planes.
- Average pooling with stride 3 (kernel size is 4, no padding), output resolution 2×2 . (ReLU)



Figure 12: The generated videos from the diffusion model Seer given the initial images as well as task descriptions.

We use the 1M replay buffer trained from vanilla DrQ-v2 for each task and collect them together as the dataset.

Distilling Diffusion Policy Foundation Models We use the fine-tuned VLM Seer to collect 100 videos for each task (1000 in bin-picking-v2), and use the trained inverse dynamics model $\rho(s_t, s_{t+1})$ to label pseudo actions for the videos. The example of generated videos is illustrated in Fig. 12. Then, we do supervised learning to train the policy foundation prior model under the dataset, which is conditioned on the task. For convenience, we encode the task embedding as a one-hot vector, which labels the corresponding task. Thus, the size of the task embedding is 8. Here, the architecture of the distilled policy model is as follows, where the downsample model is the same as that in the inverse dynamics model.

- Takes inputs as s_t, e_t , with the shape of $3 \times 84 \times 84$ and 1×8 .
- A Downsample Model, which outputs the representation with the shape of $128 \times 2 \times 2$.
- Flatten the planes into 512-dimension vectors.
- Concat the 512 vector and the task embedding into 520-dimension vectors.
- 1 Linear layer with ReLU, which outputs the 64-dimension vectors.
- 1 Linear layer with ReLU, which outputs the 64-dimension vectors.
- 1 Linear layer with ReLU, which outputs the action dimension vectors (equal to 4).

The training hyper-parameters of the inverse dynamics model $\rho(s_t, s_{t+1})$ and the distilled policy model $M_\pi(s_t, \mathcal{T})$ are in Table 3. The hyper-parameters of training FAC agents are the same as DrQ-v2 [11].

Table 3: Hyper-parameters for Building the Policy Foundation Models in Meta-World.

Parameter	Training ρ	Training M_π
Minibatch size	256	256
Optimizer	AdamW	AdamW
Optimizer: learning rate	1e-4	5e-4
Optimizer: weight decay	1e-4	1e-4
Learning rate schedule	Cosine	Cosine
Max gradient norm	1	1
Training Epochs	50	300

A.4 Running Clock Time Analysis

A.4.1 Analysis of Extra Running Clock Time in FAC

Since it brings great performance and efficiency increases for RL by leveraging the foundation prior knowledge, it is interesting and significant to investigate the clock time of running the foundation models in practice. Here we discuss the time consumed by each part from the foundation models in real and simulation. In practice, some foundation models are accessed only at the beginning or at the final step, which results in a much smaller amortization time over the trajectory. For example, GPT-4V detects success only in the final step. To make fair comparisons, we record the running clock time per trajectory and get the amortized time per step. We set the trajectory length to 50 steps for convenience. To make clear comparisons, we conclude the operations without access to foundation models into *Normal Operation* part, and those operations with access to foundation models into *Foundation Model Operation* part. All the results are evaluated in a single 3090 GPU, and we calculate the average clock time during training among 50 trajectories on average from all the tasks.

Tab. 4 and 5 are the results of real robots and simulations concerning clock time during training. Here, **Action Move** means the process of taking actions by the robotic arm. The **Action Inference** means the inference time of the learned policy model. Notably, in the simulation, we offline distill a prior policy from the diffusion model due to the heavy time-cost of video generation (in Sec. ??). Thus, the clock time of the Diffusion Policy Prior for video generation is not included in the training time, although it is much more time-consuming than the other operations in simulation.

Generally, in both environments, the time complexity of running foundation models is about 2 times more than the vanilla setting in amortization. And the most time-consuming part is the **Action**

Table 4: **Running Time of Each Part in FAC on Real Robots.** On real robots, the most time-consuming part of the foundation model operation is generating policy code from GPT-4V. The total amortized time of foundation model operations is a little larger to the normal operations.

Clock Time on Real Robots (s)	Per Trajectory	Amontized Step
<i>Normal Operation</i>		
Action Move of the gripper in the real world	-	0.320
Action Inference from policy $\pi(a s)$	-	0.001
Total	-	<u>0.321</u>
<i>Foundation Model Operation</i>		
Code Policy Prior: policy code generation from GPT-4V	14.76	0.290
Code Policy Prior: action generation by code policy	-	0.001
Success Prior: from GPT-4V	4.48	0.089
Value Prior: value inference from VIP	-	0.013
Total	-	<u>0.393</u>

Table 5: **Running Time of Each Part in FAC on Meta-World.** In the simulation, the most time-consuming part of the foundation model operation is the value inference from VIP. The total amortized time of foundation model operations is smaller than the normal operations.

Clock Time in Simulation (s)	Per Trajectory	Amontized Step
<i>Normal Operation</i>		
Action Move of the gripper in simulation	-	0.009
Action Inference from policy $\pi(a s)$	-	0.001
Total	-	<u>0.010</u>
<i>Foundation Model Operation</i>		
Diffusion Policy Prior: video generation (done offline)	11.62	0.230
Diffusion Policy Prior: action generation	-	0.001
Success Prior: from the success model	-	0.001
Value Prior: value inference from VIP	-	0.007
Total	-	<u>0.008</u>

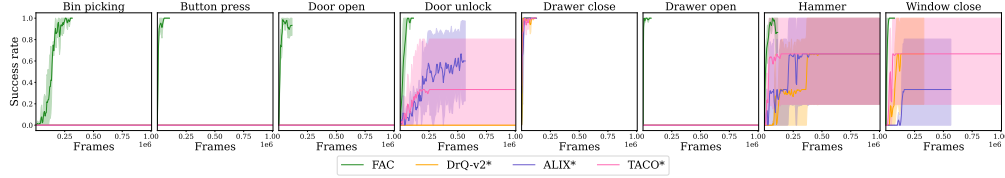


Figure 13: Here ‘*’ in DrQ-v2, ALIX, and TACO means only the 0-1 success reward is provided from the environment, which is different from the original settings in their works. FAC can work for all the tasks while the other baselines fail in half of them. It is significant and sample-efficient to utilize prior knowledge for reinforcement learning.

Move. In foundation model operations, generating the code policy from GPT-4V is the slowest on real robots, while the value inference is the slowest in simulation.

Moreover, we record the total training time spent by FAC and vanilla DrQ-v2 to make comparisons. We average the 3 seeds running for each task where we train about 100k steps on a single 3090 GPU. Vanilla DrQ-v2 takes 32m 2s on average; while FAC takes 1h 11min 17s on average, which is 2 times more than that without foundation priors. As shown in Fig. 6, even at the same clock time, FAC is better than vanilla DrQ-v2 with ground-truth rewards. FAC can solve 7/8 tasks in 100k frames, while the vanilla DrQ-v2 can only solve 2/8 in 200k frames. Furthermore, FAC can solve more tasks than the baselines. Consequently, we conclude that our method significantly outperforms the baselines concerning training clock time.

A.5 More Ablations Results

Comparison to More Baselines with Success-reward Only Here, we also add some baselines under the setting, where only the success-reward foundation prior is provided. We choose the recent SOTA model-free RL algorithms on Meta-World ALIX [70] and TACO [71], as well as the baseline DrQ-v2 [11] with the success-reward only. Notably, ALIX and TACO are both built on DrQ-v2. The results are shown in Fig. 13, where ‘*’ means that only a 0-1 success reward is given. Only FAC can achieve 100% success rates in all the environments. DrQ-v2*, ALIX*, and TACO* can not work on hard tasks such as bin-picking and door-open. FAC requires fewer environmental steps to reach 100% success rates, as shown in the Figure. The results on the new baselines can verify the significance and efficiency of utilizing the abundant prior knowledge for RL in a way.

Comprasion to BC Policies from Policy Prior Another interesting baseline of leveraging foundation policy prior is to collect success demonstrations by the prior policy M_π and train a behavior cloning policy. Here we collect 100 successful demonstrations on Meta-World for each task by the

Table 6: The performance comparison between the distilled policy prior and the learned bc policy on Meta-World.

	Prior Policy M_π	BC Policy	FAC
bin-picking-v2	0	0	1.00
button-press-topdown-v2	0.45	0.15	1.00
door-open-v2	0	0	1.00
door-unlock-v2	0	0	1.00
drawer-close-v2	0.10	0.10	1.00
drawer-open-v2	0.05	0	1.00
hammer-v2	0.15	0.10	1.00
window-close-v2	0.30	0.05	1.00

prior policy M_π . Noticing that the policy prior achieves 0% success rate on some tasks, we collect 100 trajectories then. The results are in Tab. 6. Generally, we find that the learned BC policy cannot outperform the prior policy itself in all the tasks. More significantly, in some tasks, such as windowclosev2, the BC policy achieves much worse results than the prior policy. This is because the prior policy works only in some certain scenarios, which introduces bias in the collected demos. Although the prior policy fails in some scenarios, it can introduce some informative actions, which can be much better than random actions. Therefore, it is more reasonable to leverage the prior actions as guidance for RL.

A.6 Proof of the Optimality under Policy Regularization

Lemma 1 *The policy $\pi_m = \frac{1}{1+\beta}\hat{\pi}_{\phi_m} + \frac{\beta}{1+\beta}M_\pi$, is the solution to the optimization problem of the actor shown in Equation 1.*

Proof 1 *First, $\hat{\pi}_{\phi_m}$ is the RL policy optimized by standard RL optimization problem in m -th iteration, illustrated in the following equation.*

$$\hat{\pi}_{\phi_m} = \arg \max_{\pi} \mathbb{E}_{\tau \sim \hat{\pi}_{\phi_m}} [Q(s, a)] \quad \text{as } m \rightarrow \infty \quad (4)$$

Note that the following derivation omits the variance of Gaussian distribution for convenience. This is because the variance is independent of the state in the deterministic Actor-Critic algorithms DrQ-v2 algorithm.

According to Equation 1, the policy π_m can be represented as:

$$\pi_m = \arg \min_{\pi} [-\mathbb{E}_{\tau \sim \pi} Q(s, a) + \beta \mathbf{KL}(\pi, M_\pi)] \quad (5)$$

Adding $\mathbb{E}_{\tau \sim \hat{\pi}_{\phi_m}} Q(s, a)$ in Equation 5, we can rewrite it as:

$$\pi_m = \arg \min_{\pi} [\mathbb{E}_{\tau \sim \hat{\pi}_{\phi_m}} Q(s, a) - \mathbb{E}_{\tau \sim \pi} Q(s, a) + \beta \mathbf{KL}(\pi, M_\pi)] \quad (6)$$

Considering $\mathbb{E}_{\tau \sim \hat{\pi}_{\phi_m}} Q(s, a)$ is not related to the optimization objective, the above equation holds. Intuitively, we can observe that there exist two parts in the objective. About the first part, we can use importance sampling to obtain:

$$\mathbb{E}_{\tau \sim \hat{\pi}_{\phi_m}} Q(s, a) - \mathbb{E}_{\tau \sim \pi} Q(s, a) = \mathbb{E}_{\tau \sim \hat{\pi}_{\phi_m}} \left[\frac{\hat{\pi}_{\phi_m} - \pi}{\hat{\pi}_{\phi_m}} Q(s, a) \right] \quad (7)$$

Since $\hat{\pi}_{\phi_m}$ can be represented as $\arg \max_{\pi} \mathbb{E}_{\tau \sim \pi} [Q(s, a)]$ when m approaching to infinity, the minimum of $\mathbb{E}_{\tau \sim \hat{\pi}_{\phi_m}} Q(s, a) - \mathbb{E}_{\tau \sim \pi} Q(s, a)$ can be achieved when the minimum of the following equation exists.

$$\arg \min_{\pi} \|\hat{\pi}_{\phi_m} - \pi\| \iff \arg \min_{\pi} \|\arg \max_{\pi} \mathbb{E}_{\tau \sim \pi} [Q(s, a)] - \pi\| \text{ as } m \rightarrow \infty \quad (8)$$

Let us see the second part in Equation 6. π and M_π are Gaussian distributions and the variances of distributions are constant in our framework. Thus, $\mathbf{KL}(\pi, M_\pi) \iff \|\pi - M_\pi\|$ holds.

Hereafter, we can reformulate Equation 6 as follows:

$$\pi_m = \arg \min_{\pi} [\|\arg \max_{\hat{\pi}_{\phi}} \mathbb{E}_{\tau \sim \hat{\pi}_{\phi}} [Q(s, a)] - \pi\| + \beta \|\pi - M_{\pi}\|] \quad (9)$$

Based on the Lemma 1 in [72], the solution to the above problem is derived as:

$$\pi_m = \frac{1}{1+\beta} \hat{\pi}_{\phi_m} + \frac{\beta}{1+\beta} M_{\pi} \quad (10)$$

To this end, the policy π_m is the solution to the proposed optimization problem in this paper.

Theorem 2 Let $D_{sub} = D_{TV}(\pi_{opt}, M_{\pi})$ be the bias between the optimal policy and the prior policy, the policy bias $D_{TV}(\pi_m, \pi_{opt})$ in m -th iteration can be bounded as follows:

$$\begin{aligned} D_{TV}(\pi_m, \pi_{opt}) &\geq D_{sub} - \frac{1}{1+\beta} D_{TV}(\hat{\pi}_{\phi_m}, M_{\pi}) \\ D_{TV}(\pi_m, \pi_{opt}) &\leq \frac{\beta}{1+\beta} D_{sub} \quad \text{as } m \rightarrow \infty \end{aligned} \quad (11)$$

Proof 2 Note that the following derivation is most inspired by Theorem 1 in [72]. According to Lemma 1, the policy π_m can be represented as $\frac{1}{1+\beta} \hat{\pi}_{\phi_m} + \frac{\beta}{1+\beta} M_{\pi}$.

Then, let us define the policy bias as $D_{TV}(\pi_m, \pi_{opt})$, and $D_{sub} = D_{TV}(\pi_{opt}, M_{\pi})$. Since D_{TV} is a metric that represents the total variational distance, we can use the triangle inequality to obtain:

$$D_{TV}(\pi_m, \pi_{opt}) \geq D_{TV}(M_{\pi}, \pi_{opt}) - D_{TV}(M_{\pi}, \pi_m) \quad (12)$$

According to the mixed policy definition in Equation 10, we can further decompose the term $D_{TV}(M_{\pi}, \pi_m)$:

$$\begin{aligned} D_{TV}(M_{\pi}, \pi_m) &= \sup_{(s,a) \in S \times A} \left| M_{\pi} - \frac{1}{1+\beta} \hat{\pi}_{\phi_m} - \frac{\beta}{1+\beta} M_{\pi} \right| \\ &= \frac{1}{1+\beta} \sup_{(s,a) \in S \times A} |\hat{\pi}_{\phi_m} - M_{\pi}| \\ &= \frac{1}{1+\beta} D_{TV}(\hat{\pi}_{\phi_m}, M_{\pi}) \end{aligned} \quad (13)$$

This holds for all $m \in \mathbb{N}$ from Equation 12 and Equation 13, and we can obtain the lower bound as follows:

$$D_{TV}(\pi_m, \pi_{opt}) \geq D_{sub} - \frac{1}{1+\beta} D_{TV}(\hat{\pi}_{\phi_m}, M_{\pi}) \quad (14)$$

The RL policy $\hat{\pi}_{\phi_m}$ can achieve asymptotic convergence to the (locally) optimal policy π_{opt} through the policy gradient algorithm. In this case, we can derive the bias between the mixed policy π_m and the optimal policy π_{opt} as follows:

$$\begin{aligned} D_{TV}(\pi_{opt}, \pi_m) &= \sup_{(s,a) \in S \times A} \left| \pi_{opt} - \frac{1}{1+\beta} \hat{\pi}_{\phi_m} - \frac{\beta}{1+\beta} M_{\pi} \right| \\ &= \frac{\beta}{1+\beta} \sup_{(s,a) \in S \times A} |\pi_{opt} - M_{\pi}| \quad \text{as } m \rightarrow \infty \\ &= \frac{\beta}{1+\beta} D_{TV}(\pi_{opt}, M_{\pi}) \quad \text{as } m \rightarrow \infty \\ &= \frac{\beta}{1+\beta} D_{sub} \quad \text{as } m \rightarrow \infty \end{aligned} \quad (15)$$

Therefore, we obtain the upper bound.